ICAS 2016
30th Congress of the International Council of the Aeronautical Sciences
DCC, Daejeon, Korea, September 25-30, 2016

UNCERTAINTY QUANTIFICATION AND GLOBAL SENSITIVITY ANALYSIS FOR HYPERSONIC AEROTHERMOELASTIC ANALYSIS

Kun Ye, Zhengyin Ye, Zihang Chen, Zhan Qu
National Key Laboratory of Science and Technology on Aerodynamic Design and Research, Northwestern Polytechnical University, Xi'an, Shaanxi, 710072, P.R. China

Key words *hypersonic, aerothermoelastic, uncertainty analysis, global sensitivity analysis, spare grid numerical integration, local flow piston theory*

Abstract

A novel parameterized model for temperature distribution is proposed. A framework for uncertainty quantification and global sensitivity in hypersonic aerothermoelastic analysis is developed based on this model. The uncertainty quantification and global sensitivity analysis in hypersonic aerothermoelastic analysis for control surface due to hypersonic aerothermodynamics is investigated in this study. Firstly, based on Computational Fluid Dynamics (CFD) technology, Navier-Stokes equation is solved to acquire the temperature distribution of the control surface. A parameter method based on the temperature distribution is built. Then Monte Carlo Simulation (MSC) method and Spare Grid Numerical Integration (SGNI) method are used to generate temperature distribution samples. aerothermoelastic is analyzed under the temperature distribution for all samples. The process of aerothermoelastic analysis is as following: structural modal under the effect of structure thermal stress and material property which is based on the temperature distribution samples is analyzed, structural modes is interpolated to the aerodynamic grid, aeroelasticity stability-boundary of the control surface is analyze in state space based on CFD local piston theory. Finally, the uncertainty quantification and global sensitivity analysis of aerothermoelasticity is analyzed. The framework is applied in two hypersonic flow cases. The analysis results show that: the variation coefficients of structure natural frequency and flutter analysis are 5.83%, 8.84% under the two cases, And the global sensitivity of the two uncertainty parameter is about 50% under the two cases. And the coupling of two parameters is about 0. Comparing with MCS method, SGNI method improved the efficiency of uncertainty analysis significantly.

1 Introduction

For air-breathing hypersonic vehicles, flying at high speeds will cause severe aerodynamic heating, which results in the heated structure and produces temperature gradients. High temperature will degrade material properties, while temperature gradients will produce thermal stresses. Thus Stiffness and natural frequency of the structure will change, which finally affects aerothermoelastic characteristics of the aircraft. Therefore, hypersonic aerothermoelastic is becoming an active area of research in recent years [1-6].

There are many research results about this class of problems. Culler et. al [7] established a two-way-coupling approach for aerothermo -elastic combing the third order local flow piston theory for calculating aerodynamic forces [8] and the Eckert reference enthalpy method [9] for calculating the aerodynamic heating. And the

approach was applied in aerothermoelastic analyses of the control surface and the panel of hypersonic vehicles respectively. Lamorte et. al investigated the effect of the real-gas model and the turbulence on aerothermoelastic, and they found that the transition location and the thermal stresses have obvious nonlinear influence on the aerothermoelastic analysis of control surfaces [10]. Crowel and Falkiewicz et. al studies reduced-order models for aerothermoelastic, and established a reduced-order model for calculating transient heat conduction based on the POD method [11,12]. Crowell established a reduced-order model for aerodynamic heating in hypersonic aerothermoelastic based on the Kriging method and the POD method respectively, the results demonstrated that computational efficiency is improved remarkably and the heat flux distribution has less than 5% maximum error relative to computational fluid dynamics [12]. Yang et. al proposed a aerothermal-aeroelastic two-way coupling method for hypersonic curved panel flutter, compared with the results of aerothermal-aeroelastic one-way coupling, it was revealed that the results of two-way coupling is more dangerous [13]. The effects of temperature and the structural supporting conditions on aerothermoelastic systems were considered by Wu et. al [14].

Predicting aerodynamic heating accurately is still a challenging question owing to the real-gas effect, chemical reactions and viscous interference in the hypersonic flow, which complicate the flow characteristics [15-16]. Bose et. al assessed uncertainty of hypersonic aerothermodynamics prediction capability in detail [17,18,19]. Uncertainty quantication of radiative heat flux modeling for titan atmospheric entry was studied by Ghaffari et. al [20]. In present, there are mainly three approaches to study hypersonic aerodynamic heating：(1) Wind-tunnel tests, which are very costly. Considering present conditions, it is difficult to build a hypersonic wind-tunnel meeting demands of high speed and high enthalpy [17]. Because of the model error and the sensitivity limitations of the measuring equipment, the results may have uncertainty to a certain degree sometimes. Shigeru investigated the uncertainty of aerodynamic heating in wind-tunnel tests [21]. (2) Engineering computing method for aerodynamic heating, which consists of two common methods called the reference temperature method and the reference enthalpy method. Although the engineering calculation has high computational efficiency, it ignores many influential factors in practice [22]. (3) Solving NS equations to get aerodynamic heating, which has a very high computational price, is affected by many factors such as girds, turbulence modeling, computational schemes and the real-gas model. In addition, computational results have some uncertainty [23-24]. Weaver et.al [23] and Hosder et. al [24] found that uncertainty of freestream parameters like freestream velocity, viscosity coefficient or freestream density has obvious influence on aerodynamic heating. Therefore, aerodynamic heating obtained from wind-tunnel tests or numerical simulations has certain degree of uncertainty on the one hand and the fluctuations of freestream parameters can also lead to uncertainty of aerodynamic heating on the other hand.

In aerothermoelastic analysis, aerodynamic heating is the foundation of heat conduction analysis. Thus the uncertainty of aerodynamic heating will influence the uncertainty of structure temperature distribution, which may have a negative effect on the reliability of aerothermoelastic analysis. So studying the influence of the uncertainty of aerodynamic heating on aerothermoelastic is a meaningful subject. There are many research findings about the uncertainty analysis of aeroelasticity.

Lamorte et. al examined the aeroelastic stability of a typical section representative of a control surface on a hypersonic vehicle and investigated the influence of uncertainty associated with the natural bending and torsional frequencies on aeroelasticity [25]. And they also found that uncertainty due to the location of transition from laminar to turbulent flow and the heat flux prediction has an influence on the stability of an aerodynamically heated panel. Danowsky et. al investigated the influence of the uncertainty of Mach number, height and structure parameters on wing flutter characteristics [26]. However, so far there are little literatures about the effect of uncertainty of aerodynamic heating on three dimensional structure aerothermoelastic according to the author's investigations.

The sparse grid technique, which is extend one-dimensional formulae to higher dimensions by tensor product and then select the sampling points by Smolyak theory [27], has been widely used for numerical integration and interpolation [28-29]. Recently, the sparse grid method is used for UQ (Uncertainty Quantification) and GSA (Global Sensitivity Analysis). Xiong develop a new sparse grid based method for UQ [30], which extend SPNI (Sparse Grid Numerical Integration) to moment estimations (mean or variation) and can improve accuracy and reduce computational costs for high-dimension problems with interactions of random variables. Wei developed the SPNI to importance analysis for models [31]. In this paper, the sparse grid method is used in the UQ and GSA, because its advantages: (1).the tensor product make it better suited to solve problems with highly nonlinear and strong random variable interaction. (2).the computational efficiency incerase significantly for high order non-linearities or high dimension problem. (3).When the collection points are selected, the weights are computed by sparse grid theory, for the UQ of the flow field,we need not to establish surrogate model of each grid and couple the function value to compute the corresponding weights. (4). The method is a Non-instructive method and model independent.

Aerothermoelastic is a coupling problem associated with many complicated disciplines. It is still a very complex problem. So in this study, the uncertainty of aerodynamic heating is regarded as the uncertainty of temperature distribution after heat conduction process approximately. Based on this assumption, a novel parameterized model for temperature distribution is proposed. A framework for uncertainty quantification and global sensitivity in hypersonic aerothermoelastic analysis is developed based on this model. The framework is applied in two hypersonic flow cases. Meanwhile, Monte Carlo Simulation (MCS) method and Spare Grid Numerical Integration (SGNI) method is used in uncertainty and global sensitivity analysis. And the accurate efficiency of MCS method and SGNI method is comparing.

2 Analysis Method

A novel parameterized model for temperature distribution is proposed. A framework for uncertainty quantification and global sensitivity in hypersonic aerothermoelastic analysis is developed based on this model. Uncertainty and global sensitivity analysis require a large number of samples based on the Monte Carlo method, and structure heat transfer analysis will be time-consuming, therefore the computational cost is high. It is observed that the stable structure temperature distribution after heat transfer process is similar to the surface temperature distribution in heat transfer process, which can mainly attribute to the fact that the hypersonic control surface is always thin. Therefore, the uncertainty of aerodynamic heating is regarded as the uncertainty of the temperature distribution in order to compute and analyze easily. In this

paper, two hypersonic flow cases are analyzed and compared. The framework of uncertainty and global sensitivity analysis on aerothermodynamics of hypersonic control surface aerothermoelastic is as follows:

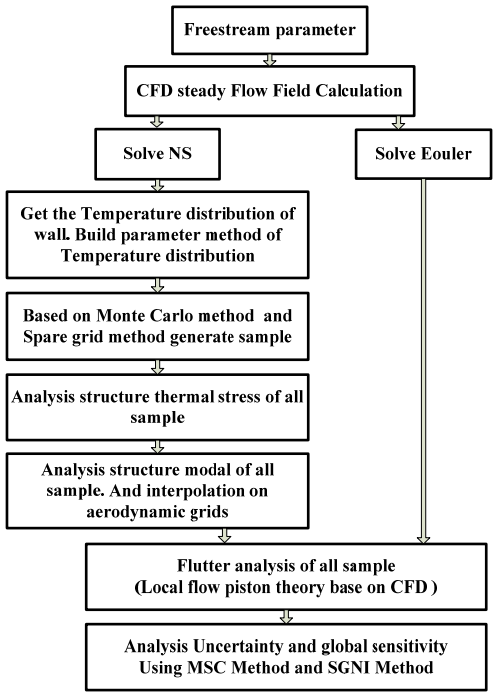

Fig. 1 The framework of uncertainty and global sensitivity analysis of aerothermoelasticty

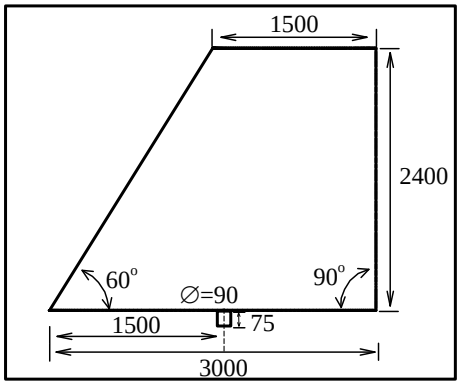

(a) The model

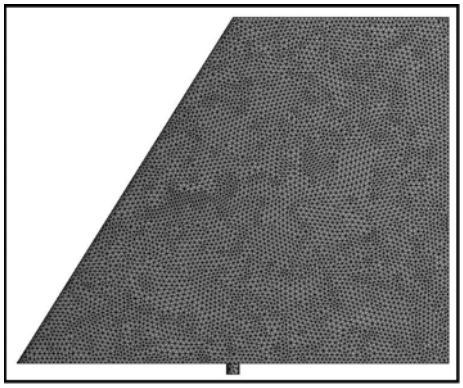

(b) The FEM mesh of the model

Fig. 2 The model and FEM mesh of the control surface (unite: mm)

2.1 Parameter Method of the Temperature Distribution

2.1.1 Computational Models

As showed in Fig. 2, the computational model used in this paper is a three dimensional all-moved control surface. Because the heat flux is inversely proportional to leading edge radius in hypersonic flow, the hypersonic vehicle and its components are always blunt. In order to analyze easily, the wing section of the control surface is NACA0005 which has a blunt leading edge. The whole control surface is connected with the fuselage by a rudderpost. The constraint conditions for the structural finite element analysis is settled as follows: the root plane of the rudderpost is fixed， the control surface structure is solid. And the structure is assumed to be made from 2024-T3 aluminum alloy.

2.1.2 Parameter Method

In order to investigate the influence of the uncertainty of the temperature distribution on the aerothermoelastic, a parameter method for the temperature distribution should be designed firstly. Crowell adopted a second-order fully polynomial to describe the temperature distribution in the literature [11]. The method needs six parameters to control the function, like equation (1) shows. However, there are two deficiencies when applying the method to the uncertainty analysis：1) Too many parameters may lower the computational efficiency because the Monte Carlo Simulation method needs lots of samples. 2) The meanings of six parameters in the second-order polynomial are not clear enough to describe the temperature distribution. The parameter b_1 translates the function up and down. The parameters $b_2 \sim b_6$ control the slope of the function in varying degrees, so it is

difficult to distinguish them. Therefore, it is difficult to derive a clear conclusion when using these six parameters to analyze the uncertainty.

$$T_s(x,y,t) = b_1(t) + b_2(t)x + b_3(t)y + b_4(t)x^2 + b_5(t)xy + b_6(t)y^2 \quad (1)$$

Because the wing section of the control surface is symmetric, and the angle of attack is 0 degree, so the distribution of the aerodynamic heating is also symmetric. Under the condition of M=6 and H=15km, the contour of the temperature distribution and the temperature distribution of three sections along the spanwise direction are illustrated in the Fig. 3. And x axis is chordwise direction and z axis is spanwise direction. It can be seen from the Fig. 3 that the variations of temperature distribution in different sections stay basically the same. And so the leading edge stagnation point temperatures and the profiles of the temperature distribution in all the sections do. So fitting the temperature distribution of the root section to get the fitting function, and normalizing other sections along the spanwise direction, then the temperature distribution on the whole control surface is obtained. The Fig. 4 shows the temperature distribution after function fitting. It can be seen that the Fig. 4 is similar to the Fig. 3(a), which proves that this parameter method is feasible.

The fitting function is:

$$f(X) = \frac{p_1 X + p_2}{X + p_3} \quad (2)$$

The transition function for normalizing is:

$$X(x,z) = \frac{x - az}{1 - az} \quad (3)$$

The final expression of the function is:

$$f(x,z) = \frac{p_1(x - ax)/(1 - az) + p_2}{(x - ax)/(1 - az) + p_3} \quad (4)$$

In terms of aerodynamic heating, the reason for getting similar heat flux or temperature distribution by different ways is mainly the divergence of the distribution profile slopes and the stagnation point temperatures. In terms of the structure, temperature affects material properties, while temperature gradients (corresponding to the profile slope) produce thermal stresses, thus the structure stiffness changes. Based on the conclusions above, two ways of disturbing $f(x,z)$ are adopted to get parameters of uncertainty analysis. (1) Translate $f(x,z)$ up and down; (2) Change the slope of $f(x,z)$ in the condition that the stagnation temperature stays constant. It is found that the parameter p_1 in $f(x,z)$ can control the slope of the function well and the parameters p_2 and p_3 cannot translate the function up and down easily. Therefore, a new parameter q_1 is introduced. The function $f(x,z)$ is added q_1 and reduced b.

$$f(x,z) = \frac{p_1(x - ax)/(1 - az) + p_2}{(x - ax)/(1 - az) + p_3} + q_1 - b \quad (5)$$

In the equation (5), $q_1 = b$, it is easier to translate the function up and down by adjusting q_1, and the value of the parameter b is equal to leading edge stagnation point temperature.

Therefore, the parameters p_1 and q_1 are extracted as uncertainty parameters to control the temperature distribution. The function of the parameter p_1 is to control the profile slope of the temperature distribution. The function of the parameter q_1 is to control the stagnation point temperature. And the influence of the uncertainty of the temperature field on the aerothermodynamics is investigated in the next. The Fig. 5(a) shows the results when plus or minus 20% disturbances are imposed on the parameter p_1, while the Fig. 5(b) shows the results when plus or minus 10% disturbances are imposed on the parameter q_1.

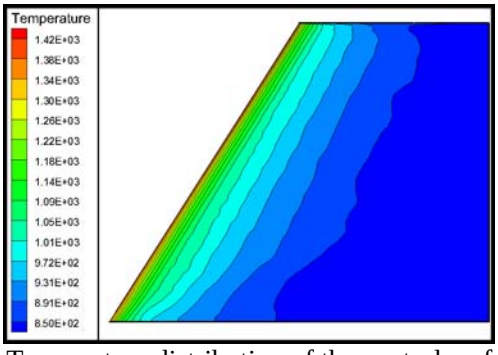

(a) Temperature distribution of the control surface

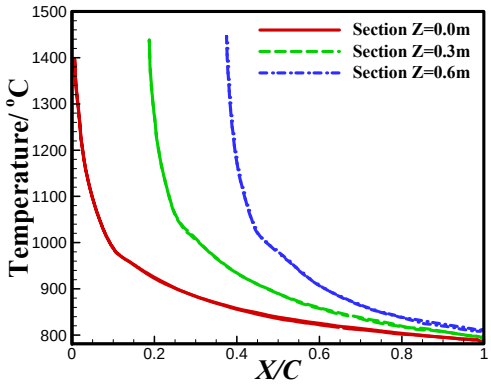

(b) Temperature distribution of three sections

Fig. 3 The temperature distribution of the control surface and three sections

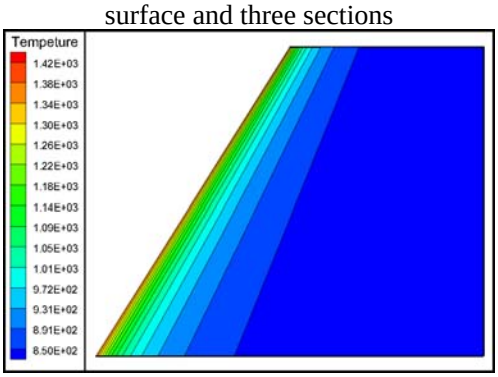

Fig. 4 The parameterized temperature distribution

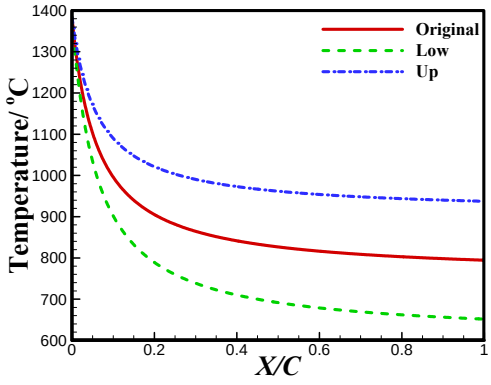

(a) Slope disturbance

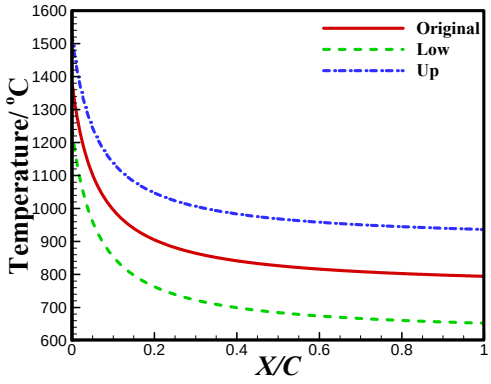

(b) Translation disturbance

Fig. 5 Disturbance of uncertainty parameters

2.2 Uncertainty Analysis Method

The Monte Carlo Simulation (MCS) method that is common in uncertainty analysis is applied firstly [32]. Then the Spare Grid Numerical Integration (SGNI) method which is becoming more common in uncertainty analysis in recent years is used.

2.2.1 The SGNI Method

In recent years, the SGNI method based on the Smolyak criterion has been widely applied. The basic thought is to use combinations of tensor products of suitable one-dimensional formulas to construct multivariate quadrature formulas [33-35]. Compared to direct combinations of tensor products, the computational load and accuracy are no longer dependent on the dimension of input variables exponentially. The basic idea of the SGNI method is given in the next.

U_1^{ij} and $w_1^{i_j}$ are assumed to stand for the integration point and the weight of the one dimensional space of the jth variable respectively. The set of all spare grid numerical integration points with the degree of accuracy k in the n dimensional space, U_n^k , are selected according to Smolyak criterion ：

$$U_n^k = \bigcup_{k+1\le|i|\le q} U_1^{i_1} \otimes U_2^{i_2} \otimes \ldots \otimes U_d^{i_n} \tag{6}$$

In the equation (6)， $\otimes$ stands for the calculation of tensor product， $q = k + n$， $|i| = i_1 + i_2 + \cdots + i_n$ are the sum of the multidimensional index. In order to remove the grid points which have little effect on computational accuracy, a limitation is settled as $k+1 \le |i| \le q$. According to the Smolyak criterion，the weight w_l of the lth integration point $\xi_l = \left[\xi_{j_{i_1}}^{i_1}, \xi_{j_{i_2}}^{i_2}, \cdots, \xi_{j_{in}}^{i_n}\right]$ in the set U_n^k is：

$$w_l = (-1)^{q-|i|}\binom{n-1}{q-|i|}(w_{j_{i_1}}^{i_1} \cdots w_{j_{in}}^{i_n}) \tag{7}$$

The integration of the nonlinear function $g(\mathbf{x})$ including the n dimensional basic variable $x = (x_1, x_2, \cdots, x_n)$ can be obtained by the sparse grid numerical integration equations showed in (8). And the accuracy can be the same as *(2k+1)* th order polynomial.

$$\int_{-\infty}^{+\infty} g(\mathbf{x})f(\mathbf{x})d\mathbf{x} \approx \sum_{l=1}^{N_n^k} w_l g(T^{-1}(\xi_l)) = \sum_{l=1}^{N_n^k} w_l g(\mathbf{x}_l) \quad (8)$$

The parameter N_n^k stands for the number of integration points in the set U_n^k, and the function $f(\mathbf{x})$ is the joint probability density function of the variable x. The parameters ξ_l and w_l are the integration point and its weight in the n dimension space respectively, which are obtained by the sparse grid technology. The function $T^{-1}(\xi_l)$ is the inverse function of the transition function which transfers the variable x with the arbitrary distribution to the integration point space. The value of the variable x at the first integration point ξ_l is written as x_l.

The integration of output average value and variance of the model $y = g(\mathbf{x})$ can be calculated by the sparse grid numerical integration following the equation (10). And the accuracy can be the same as (2k+1) th order polynomial.

$$E_Y = \int_{-\infty}^{+\infty} g(\mathbf{x})f(\mathbf{x})d\mathbf{x} \approx \sum_{l=1}^{N_n^k} w_l g(T^{-1}(\xi_l)) = \sum_{l=1}^{N_n^k} w_l g(\mathbf{x}_l) \quad (9)$$

$$\begin{aligned} V_Y &= \int_{-\infty}^{+\infty} (g(\mathbf{x}) - E_Y)^2 f(\mathbf{x})d\mathbf{x} \\ &\approx \sum_{l=1}^{N_n^k} w_l (g(T^{-1}(\xi_l)) - E_Y)^2 \\ &= \sum_{l=1}^{N_n^k} w_l (g(\mathbf{x}_l) - E_Y)^2 \end{aligned} \quad (10)$$

The SGNI method based on the Smolyak criterion can overcome the disadvantage of transitional numerical integration whose computational costs increases exponentially with the dimension of variables. And it has a wide applicability in high-dimensional integration problems. The procedure is easy and flexible, and different types of one dimensional integration points can be chosen according to various input distributions. The integration accuracy can be improved by adjusting the degree of accuracy k.

2.2.2 Global Sensitivity Analysis

Global Sensitivity Analysis, also called importance measurement, is used to investigate the contribution of the uncertainty of input variables to the uncertainty of the model output. Because the influence of the basic variable varying in its range on the uncertainty of the output is considered synthetically, this method is widely used in the engineering design and the probabilistic safety assessment. The method using the variance to analyze the global sensitivity is effective in investigating the influence of the uncertainty of the basic variables on the uncertainty of the output. The importance influence of the fluctuations of the output variables caused by the input parameters and the cross coupling interaction among the parameters are investigated in the method. The method is used for global sensitivity analyzing in this study.

According to Sobol's dimension reduction analysis [19], the total variance can be expressed as follows:

$$V(Y) = \sum_i V_i + \sum_i \sum_{j>i} V_{ij} + \cdots + V_{12\cdots k} \quad (11)$$

$V_i = V[E(Y|X_i)], V_{ij} = V[E(Y|X_i, X_j)], \cdots$, both sides of the equation (11) are divided by $V(Y)$, the results are as follows:

$$\sum_i S_i + \sum_i \sum_j S_{ij} + \sum_i \sum_{j>i} \sum_{l>j} S_{ijl} + \ldots + S_{123\ldots k} = 1 \quad (12)$$

S_i is the main sensitivity index, $S_{ij}, S_{ijl}, \ldots, S_{123\ldots k}$ reflects the cross influence effects. The main sensitivity index can be expressed as the ratio of the output responsive expected variance to the total variance:

$$S_i = \frac{V[E(Y|X_i)]}{V(Y)} \quad (13)$$

2.2.3 Numerical Examples

There is a nonlinear function defined as $f(x_1, x_2) = x_1 \times x_2$, whose independent variables x_1, x_2 obey the norm distribution as follows: $\mu_1 = 1, \mu_2 = 2, \sigma_1 = 3, \sigma_2 = 2$. The sixth order SGNI method is adopted to analyze the uncertainty and global sensitivity of the function $f(x_1, x_2)$. The results are listed in the Table 1.

Table 1 Comparison of result of SGNI method and Analytic

	SGNI	Analytic solution
Mean	2.0000	2.000
Variance	76.000	76.00
S_{x_1}	0.4737	9/19
S_{x_2}	0.0526	1/19

S_{x_1,x_2}	0.4737	9/19

2.3 Aerothermoelastic Analysis Method

2.3.1 Fluid Control Equations

The Reynold's Averaged Navier-Stokes equations are shown as follows, which is used to calculate the steady aerodynamic heat:

$$\frac{\partial}{\partial t}\iiint_V \boldsymbol{Q}\cdot dV+\int_{\partial V}\boldsymbol{F}^c(\boldsymbol{Q})\cdot\boldsymbol{n}d\mathrm{S}=\int_{\partial V}\boldsymbol{F}^v(\boldsymbol{Q})\cdot\boldsymbol{n}d\mathrm{S} \quad (14)$$

Where $\boldsymbol{Q}=[\rho,\rho u,\rho v,\rho w,e]^T$ is the conserved variable, Ω and $\partial\Omega$ are the control volume and its boundary, ρ、u、v、w、E are the gas density、velocities in x、y and z directions. The total internal energy per unit volume, $\boldsymbol{F}^c(\boldsymbol{Q})$ and $\boldsymbol{F}^v(\boldsymbol{Q})$ are the inviscid flux term and the viscous flux term, respectively. The equations are solved by FLUENT15.0. The turbulence model is selected as *k-w* SST model. The no-slip and radiant heat equilibrium boundary condition is applied to the control surface. The Stefan-Boltzmann law correction formula is used when calculating the radiant heating:

$$q_{rad}=\sigma\varepsilon(T_w^4-T_\infty^4) \quad (15)$$

In the equation (15), ε is the external emissivity, whose value is referred as 0.8 in this paper, σ stands for the Standford constant whose value is $5.6697\times10^{-8}(w/m^2K^4)$., and the external radiation temperature T_∞ is referred as 300K. The Space mesh and the wall mesh are showed in the Fig. 6 .

When $\boldsymbol{F}^v(\boldsymbol{Q})$ =0, the equations (14) will simplify to the Euler equations. And the local flow parameters on the surface are obtained by solving the Euler equation

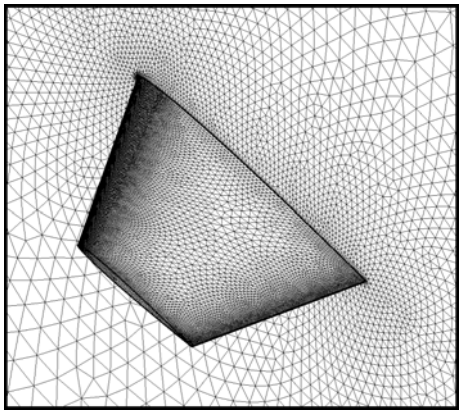

Fig. 6 The mesh of control surface

2.3.2 Modal Analysis and Interpolation

The free vibration equation of the structure with considering the temperature effects and ignoring the damping is shown as follows:

$$\boldsymbol{M}\ddot{\boldsymbol{u}}+\left(\boldsymbol{K}_s(T)+\boldsymbol{K}_\sigma(T)\right)\boldsymbol{u}=\boldsymbol{0} \quad (16)$$

Where $\boldsymbol{M}$ is the mass matrix; $\boldsymbol{K}_s(T)$ is the convention stiffness matrix that varies due to the temperature-dependence of the material properties, and $\boldsymbol{K}_\sigma(T)$ is the geometric stiffness matrix resulting from thermal stresses. And it is solved by ANASYS15.0. FEM method

When the structural temperature is 300K, the first four order natural frequencies and mode shape are shown in the Fig. 7. The Radial basis function (RBF) is used for interpolating structure modes on aerodynamic grids.

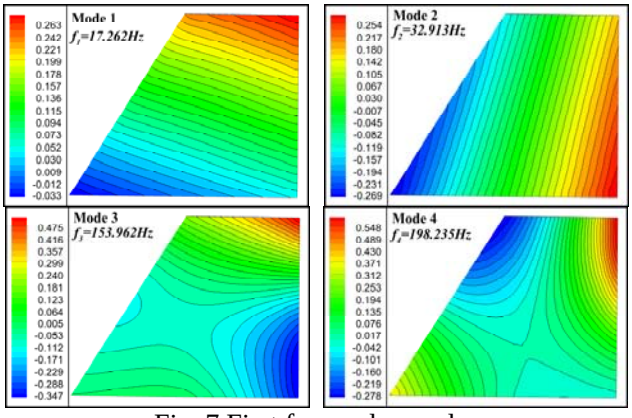

Fig. 7 First four order modes

2.3.3 Unsteady Aerodynamics Calculations and Aeroelastic Analysis

Commonly, the unsteady aerodynamics are approximated using either piston theory [5,6,7] or a similar Van Dyke second-order theory [36] , which is essentially equivalent to second-order

piston theory at hypersonic Mach numbers. The lifting surface/panel approaches have also been employed [37]. The local piston theory (LPT) is efficient and sufficiently accurate [38]. In this study, the local piston theory based on CFD is applied to calculate the unsteady aerodynamic pressure, and the general aerodynamic forces based on mode coordinates can be written as follows:

$$\boldsymbol{Q}=\frac{\rho_\infty V_\infty^2}{M_\infty}\boldsymbol{A}\boldsymbol{\xi}+\frac{\rho_\infty V_\infty}{M_\infty}\boldsymbol{B}\dot{\boldsymbol{\xi}} \tag{17}$$

In the equation (17) :

$$\boldsymbol{A}_{ij}=\iint_{wing}\left\{\sqrt{D_\rho D_p}\left[D_a D_M\cdot(\boldsymbol{n}_0-\boldsymbol{n}_j^0)\right]\left[(-\boldsymbol{n}_0)\cdot\boldsymbol{zx}_i\right]\right\}\mathrm{d}s \tag{18}$$

$$\boldsymbol{B}_{ij}=\iint_{wing}\left\{\sqrt{D_\rho D_p}\left[\boldsymbol{zx}_j\cdot\boldsymbol{n}_0\right]\left[(-\boldsymbol{n}_0)\cdot\boldsymbol{zx}_i\right]\right\}\mathrm{d}s \tag{19}$$

$$D_p=\frac{p_l}{p_\infty},\quad D_\rho=\frac{\rho_l}{\rho_\infty},\quad D_a=\frac{a_l}{a_\infty},\quad D_M=\frac{M_l}{M_\infty} \tag{20a~20d}$$

Where ρ_∞、V_∞、M_∞、p_∞、a_∞ are the density、the velocity、the Mach number 、the pressure and the speed of the freestream, respectively. ρ_l、V_l、M_l、p_l、a_l are the relative parameter of the local flow; $\boldsymbol{n}_0$ is the unit vector outward normal to the wall before deformation, $\boldsymbol{n}_j^0$ is the unit vector outward normal to the wall of the j^{th} mode after unit deformation, $\boldsymbol{zx}_j$ is the j^{th} mode of vibration of the corresponding point, $\boldsymbol{\xi}$ is the generalized coordinate.

For a specific computational case, $\boldsymbol{A}$ and $\boldsymbol{B}$ are determined by solving the Euler equations and obtaining the steady flow field. The aerodynamic force coefficient matrix based on mode coordinates as equation. (17) could be coupled with the structural equations of motion to perform an aeroelastic analysis.

2.3.4 Aeroelastic Analysis

Based on Lagrange equations, the final equations of motion can be written as follows:

$$\boldsymbol{M}\ddot{\boldsymbol{\xi}}+\boldsymbol{G}\dot{\boldsymbol{\xi}}+\boldsymbol{K}\boldsymbol{\xi}=\boldsymbol{Q} \tag{21}$$

Where $\boldsymbol{M}$ is the mass matrix, $\boldsymbol{G}$ is the structural damping matrix, $\boldsymbol{K}$ is the stiffness matrix, $\boldsymbol{Q}$ is the generalized aerodynamic force matrix. $\boldsymbol{G}$ is difficult to obtain from experiments and numerical simulation, so we assumed $\boldsymbol{G}=\boldsymbol{0}$ in this paper. Substitute equation.(20) into equation. (21) we have

$$\boldsymbol{M}\ddot{\boldsymbol{\xi}}+\boldsymbol{K}\boldsymbol{\xi}=\frac{\rho_\infty V_\infty^2}{M_\infty}\boldsymbol{A}\boldsymbol{\xi}+\frac{\rho_\infty V_\infty}{M_\infty}\boldsymbol{B}\dot{\boldsymbol{\xi}} \tag{22}$$

Where $\boldsymbol{x}_s=\left[\xi_1,\xi_2,\cdots,\xi_N,\dot{\xi}_1,\dot{\xi}_2,\cdots,\dot{\xi}_N\right]^T$, then flutter equation can be written as:

$$\dot{\boldsymbol{x}}_s=\boldsymbol{C}\cdot\boldsymbol{x}_s \tag{23}$$

Where

$$\boldsymbol{C}=\begin{bmatrix}0 & \boldsymbol{I}\\ \boldsymbol{M}^{-1}\left(\frac{\rho_\infty V_\infty^2}{M_\infty}\boldsymbol{A}-\boldsymbol{K}\right) & \frac{\rho_\infty V_\infty}{M_\infty}\boldsymbol{M}^{-1}\boldsymbol{B}\end{bmatrix} \tag{24}$$

For a given M_∞、V_∞、ρ_∞, $\boldsymbol{C}$ is a real matrix, so the stability analysis of the aeroelastic system is transformed into solving the eigenvalue of matrix $\boldsymbol{C}$ in state equation. The frequencies and damping of the aeroelastic system are given by the eigenvalues. The frequencies and corresponding damping coefficients are uniquely identified by the real and imaginary parts of the eigenvalues. When the real part of the eigenvalues crosses the imaginary axle, the stability of system will change. The derivation details and verification samples are illustrated in the literature [38].

3 Calculation Results and Analysis

For the all-moved control surface model in this study, the uncertainty effect of the aerodynamic heating on aerothermoelastic is investigated under two flight conditions which are M=5， H=15km， Alfa=0° and M=5， H=15km，Alfa=0°.

3.1 The Results for the Condition 1

The free stream parameters are as follows：M=5，H=15km，Alfa=0° . The values of the parameters in temperature distribution function are listed as follows:

$$p_1=625.5,\quad p_2=74.86,\quad p_3=0.07483,$$
$$q_1=1010,\quad a=0.625,b=1010$$

The statistic characteristic of uncertainty parameters p_1 and q_1 are listed in the Table 2. The value of the coefficient of variation of the parameter p_1 is 0.2， and the value of the coefficient of variation of the parameter q_1 is

0.1. In the condition, the maximum fluctuation of two parameters on the temperature is 101 K. When analyzing the global sensitivity, the influence of the parameters p_1 and q_1 on the function can be seen as in the same level. That is similar in the condition 2.

Table 2 Static property of the uncertainty parameters

	Distribution	Mean	Standard deviation	Variation coefficient
p_1	Normal	625.50	125.10	0.20
q_1	Normal	1010.00	101.00	0.10

The MCS method and the SGNI method are adopted to analyze the uncertainty and global sensitivity of the issue. In order to analyze as accurate as possible, the sample number of the MCS method is 20000 and the SGNI method has tenth-order accuracy. In the SGNI method, the number of integration points for uncertainty analysis is 381 and the number of integration points for global sensitivity is 200.

The probability density distribution of the vibration velocity from the MCS method is showed in the Fig. 8. The cumulative probability density distribution of the vibration velocity from the MCS method is showed in the Fig. 10. The results of uncertainty and global sensitivity of aerothermoelastic from the MCS method or the SGNI method are illustrated in the Table 4 and the Table 3 respectively. It is obvious that the results from two different methods are similar. But the number of samples which the SGNI method requires is much smaller than that which the MCS method requires. The conclusion can be derived from the results that the variation coefficients of the specific parameters (including first order frequency, second frequency, and the difference between the first and second frequency, the vibration velocity and the frequency) are all similar. Their value is all 5.82% around. So the influence of the uncertainty of the temperature distribution on structure stiffness is coincident with that on the flutter analysis. The sensitivity of the parameter p_1 is 0.535，and the sensitivity of the parameter q_1 is 0.464. It is said that the influences on the flutter results from the parameters p_1 and q_1 are similar. The value of the parameter p_1 is a little higher than the parameter q_1. The value of the global sensitivity of the coupling reaction between the parameter p_1 and the parameter q_1 is 0.0003， which is very small. So the coupling effect can be basically ignored.

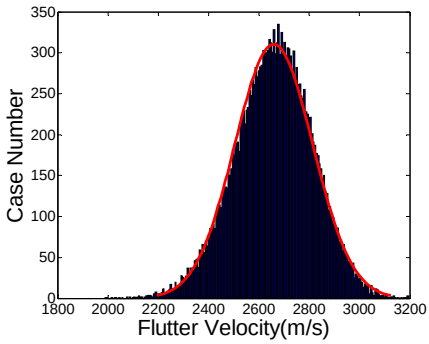

Fig. 8 Probability density of flutter velocity

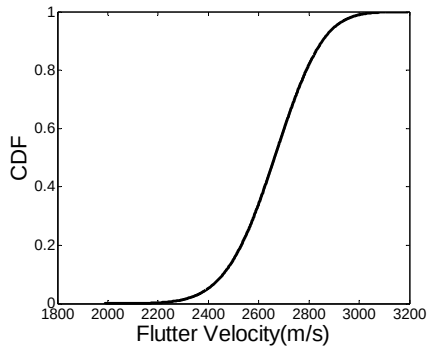

Fig. 9 Cumulative probability density of flutter velocity

Table 3 Uncertainty and global sensitivity analysis results of MCS method

	First order frequency/Hz	Second order frequency/Hz	Frequency Space/Hz	Flutter Velocity/(m/s)	Flutter Frequency/Hz
Mean	13.65000	26.17650	12.52420	2658.930	20.20250
Standard deviation	0.794240	1.523856	0.729612	154.8183	1.175972
Variation coefficient	0.058186	0.058215	0.058256	0.058226	0.058209
S_{p_1}	0.535522	0.533532	0.531452	0.537561	0.537217
S_{q_1}	0.464160	0.462959	0.461866	0.461689	0.462682
$S_{p_1-q_1}$	0.000318	0.003509	0.006682	0.000750	0.000101

Table 4 Uncertainty and global sensitivity analysis results of SGNI method

	First order frequency/Hz	Second order frequency/Hz	Frequency Space/Hz	Flutter Velocity/(m/s)	Flutter Frequency/Hz
Mean	13.13731	13.65212	12.52656	2659.630	20.20569
Standard deviation	0.766750	0.795296	0.730689	154.9090	1.172990
Variation coefficient	0.058364	0.058254	0.058331	0.058243	0.058052
S_{p_1}	0.535402	0.533328	0.535956	0.536674	0.541039
S_{q_1}	0.459848	0.461853	0.459511	0.460673	0.456359
$S_{p_1-q_1}$	0.004750	0.004819	0.004533	0.002653	0.002602

3.2 The Results for the Condition 2

The free stream parameters are as follows: M=6， H=15km， Alfa=0. The values of the parameters in temperature distribution function are listed as follows:

$$p_1 = 758.3, p_2 = 84.92, p_3 = 0.06138$$

$$q_1 = 1421, a = 0.625, b = 1421$$

The statistic characteristic of uncertainty parameters p_1 and q_1 are listed in the Table 5.

Table 5 Statistic property of uncertainty parameters

	Distribution	Mean	Standard deviation	Variation coefficient
p_1	Normal	758.30	151.66	0.20
q_1	Normal	1421.00	142.10	0.10

The probability density distribution of the vibration velocity from the MCS method is showed in the Fig. 10. The cumulative probability density distribution of the vibration velocity from the MCS method is showed in the Fig. 11. The results of uncertainty and global sensitivity of aerothermoelastic from the MCS method or the SGNI method are illustrated in the Table 6 and the Table 7 respectively. The conclusion can be derived from the results that the variation coefficients of the specific parameters (including first order frequency, second frequency, and the difference between the first and second frequency, the vibration velocity and the frequency) are all similar. Their value is all 8.83% around. So the influence of the uncertainty of the aerodynamic heating on the structure frequency and the flutter properties is obvious. When designing the structure, the influence of the uncertainty of the aerodynamic heating should be considered.

Compared to the condition 1， the degree of the variations of the structure frequency or the flutter analysis results is higher with the same degree of the variations of the uncertainty parameters. The sensitivity of the parameter p_1 is 0.4726，and the sensitivity of the parameter q_1 is 0.525. Compared to the condition 1, the global sensitivity of the parameter p_1 deceases slightly, and the global sensitivity of the parameter q_1 increases slightly. The value of the global sensitivity of the coupling reaction between the parameter p_1 and the parameter q_1 is 0.0002, which is still very small.

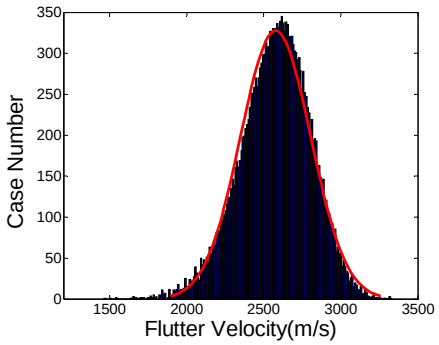

Fig. 10 Probability density of flutter velocity

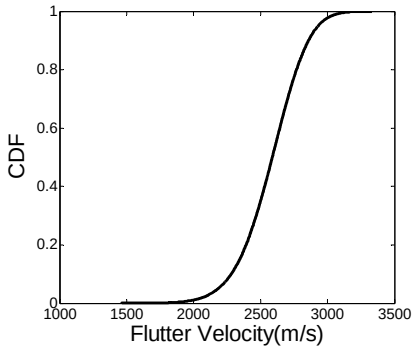

Fig. 11 Cumulative probability density of flutter velocity

Table 6 Uncertainty and global sensitivity analysis results of MCS method

	First order frequency/Hz	Second order frequency/Hz	Frequency Space/Hz	Flutter Velocity/(m/s)	Flutter Frequency/Hz
Mean	12.77978	24.51119	11.72958	2576.520	18.64778
Standard deviation	1.130163	2.167413	1.037249	227.6000	1.647405
Variation coefficient	0.088434	0.088425	0.088430	0.088338	0.088343
S_{p_1}	0.472670	0.473719	0.474567	0.472425	0.472719
S_{q_1}	0.525122	0.524199	0.523115	0.525686	0.525614
$S_{p_1-q_1}$	0.002208	0.002082	0.002318	0.001889	0.001667

Table 7 Uncertainty and global sensitivity analysis results of SGNI method

	First order frequency/Hz	Second order frequency/Hz	Frequency Space/Hz	Flutter Velocity/(m/s)	Flutter Frequency/Hz
Mean	12.77103	24.51650	11.72890	2576.470	18.64817
Standard deviation	1.132696	2.171439	1.037261	227.9300	1.648742
Variation coefficient	0.088692	0.088570	0.088435	0.088465	0.088413
S_{p_1}	0.469838	0.471876	0.474481	0.471181	0.471815
S_{q_1}	0.522871	0.522641	0.523545	0.524165	0.524318
$S_{p_1-q_1}$	0.007291	0.005483	0.001974	0.004654	0.003867

4 Comparison of Computational Efficiency

There is a comparison of computational efficiency when different methods are applied into the analysis of the uncertainty and the global sensitivity in the Table 8. The time data in the table are all obtained with only one CPU running. The whole procedures are program-controlled automatic. Two quad-core computers (CPU dominant frequency is 4.00 GHz) are used. It costs 11 days to finish the whole computational process. Most of the time is spent on the MSC method. Although a lot of the samples are used in the MSC method, the results from the tenth order SGNI method are similar to that from the MSC method. Besides that, the computational efficiency improves more than 50 times compared to the MSC method. So the SGNI method is proved to be an effective uncertainty analysis method.

Table 8 Comparison of efficiency between MCS method and SGNI method

Method	Uncertainty Analysis		Global Sensitivity Analysis	
	Number of Sample	CPU time/h	Number of Sample	CPU time/h
MCS	20000	220	30000	330
SGNI	381	4.19	200	2.20

5 Conclusions

By investigating the effect of aerodynamic heating uncertainty in hypersonic aerothermoelastic, some conclusions can be obtained as follows：

(1) A suitable parameter model for the temperature distribution is proposed. Its number of parameters is only two and it can describe two important disturbances of the temperature distribution.

(2) Under two different flight conditions, the MCS method and the SGNI method are used to analyze the uncertainty and the global sensitivity of the temperature distribution. The results show that under given uncertainty parameters， 1)

M=5，H=15km，the variation coefficients of natural structure frequency and the flutter analysis results are 5.83%. 2) M=6，H=15km, the variation coefficients of natural structure frequency and the flutter analysis results are 8.84%. So the influence of the uncertainty of the aerodynamic heating on the structure frequency and the flutter properties is obvious. When designing the structure, the influence should be considered.

(3) In two different flight conditions, the values of the global sensitivity of the two uncertainty parameters are all about 50%. The coupling effect between two parameters is very small.

(4) The results from two different methods are almost identical, but the SGNI method is more efficient than the MCS method.

Acknowledgements

The authors acknowledge the financial support of the National Key Laboratory of Aerodynamic Design and Research Foundation of China and the support of National Natural Science Foundation of China (NSFC) under grant NO. 91216202

Referencess

[1] Klock R J, Cesnik C E S. Aerothermoelastic smulation of air-breathing hypersonic vehicles. Aiaa/asme/asce/ahs/sc Structures, Structural Dynamics, and Materials Conference. AIAA Paper, 2014-0149, 2014.

[2] Bertin, J J, and Cummings, R M. Fifty years of hypersonics:where we've been, Where We're Going. Progress in Aerospace Sciences, Vol. 39, No. 6–7, pp. 511–536, 2003

[3] McNamara J J, Friedmann P P. Aeroelastic and aerothermoelastic analysis in hypersonic flow: past, present, and future. AIAA Journal, Vol. 49, No. 6, pp. 1089–1122, 2011

[4] Fidan B, Mirmirani M, Ioannou P A. Flight Dynamics and Control of Air-Breathing Hypersonic Vehicles: Review and New Directions. Proceedings of the 12th AIAA International Space Planes and Hypersonic Systems and Technologies, AIAA Paper 2003-7081, 2003.

[5] McNamara J J, Friedmann P P. Three-dimensional aeroelastic and aerothermoelastic behavior in hypersonic flow. AIAA Paper, 2005-2175, 2005

[6] McNamara J J, Friedmann P P, Powell K, Thuruthimattam B, and Bartels R. Aeroelastic and aerothermoelastic behavior in hypersonic flow. AIAA Journal, Vol. 46, No.10, pp. 2591–2610, 2008

[7] Culler A J, McNamara J J. Studies on fluid-thermal-structural coupling for aerothermoelasticity in hypersonic flow. AIAA Journal, Vol. 48, No.8, pp. 1721-1738, 2010

[8] Ashley H, and Zartarian G. Piston theory—a new aerodynamic tool for the aeroelastician. Journal of the Aeronautical Sciences, Vol. 23, No. 12, pp. 1109–1118, 1956

[9] Eckert E R G. Engineering relations for heat transfer and friction in high-velocity laminar and turbulent boundary-layer flow over surfaceswith constant pressure and temperature. Transactions of the ASME, Vol. 78, No.6, pp.1273–1283, 1956

[10] Lamorte N, Friedmann P P. Hypersonic aeroelastic and aerothermoelastic studies using computational fluid dynamics, AIAA Journal, Vol. 52, No.9, pp.2062-2078, 2014

[11] Crowel A R, McNamara J J. Model reduction of computational aerothermodynamics for hypersonic aerothermoelasticity. AIAA Journal, Vol. 50, No.1, pp.74-84, 2012

[12] Falkiewicz N, Cesnik C E S, Crowell A R, McNamara, J J. Reduced-order aerothermoelastic framework for hypersonic vehicle vontrol simulation. AIAA Journal, Vol. 49, No.8, pp.1625-1646, 2011

[13] Yang C, Li G S, Wan Z Q. Aerothermal-aeroelastic two-way coupling method for hypersonic curved panel flutter. Science China Technological Sciences, Vol. 55, No.3, pp. 831-840, 2012

[14] Wu Z G, Hui J P, Yang C. Hypersonic aerothermoelastic analysis of wings. Journal of Beijing University of Aeronautics & Astronautics., Vol. 3, No.3, pp.270-273, 2005

[15] Bertin J J. Hypersonic aerothermodynamics, AIAA, Reston, VA, 1994.

[16] Anderson J D. Hypersonic and high-temperature gas dynamics, 2nd ed., AIAA, Reston, VA, 2006.

[17] Bose D, Brown J L, Prabhu D K, et al. Uncertainty assessment of hypersonic aerothermodynamics prediction capability. Journal of Spacecraft and Rockets, Vol. 5050, No.1, pp.12-18, 2013

[18] Bose D, Wright M J, and Palmer G. Uncertainty analysis of laminar aeroheating predictions for mars entries. Journal of Thermophysics and Heat Transfer, Vol. 20, No. 4, Oct.–Dec, pp. 626–662, 2006

[19] Bose D, Wright M, and Gökçen T. Uncertainty and sensitivity analysis of thermochemical modeling for titan atmospheric entry. 37th AIAA Thermophysics Conference, AIAA Paper 2004-2455, Portland, OR, 2004

[20] Ghaffari S, Magin T, and Iaccarino G. Uncertainty quantication of radiative heat flux modeling for titan atmospheric entry. AIAA Paper 2010-239, 48th AIAA Aerospace Sciences Meeting, Orlando, FL, 4–7 Jan. 2010.
[21] Shigeru K I. Uncertainty evaluation of thermocouple aeroheating measurements for hypersonic wind-tunnel tests. Journal of Spacecraft and Rockets, Vol. 43, No.3, pp.698-700, 2006
[22] Bettis B, and Hosder S. Efficient uncertainty quantification approach for reentry flows with mixed uncertainties. Journal of Thermophysics and Heat Transfer, Vol. 25, No. 4, pp. 523–535, 2011
[23] Weaver A B, Alexeenko A A, Greendyke R B, et al. Flow field uncertainty analysis for hypersonic CFD simulations. Aiaa Aerospace Sciences Meeting Including the New Horizons Forum and Aerospace Exposition.AIAA Paper, 2010-1180, 2010
[24] Hosder S, Bettis B R. Uncertainty and sensitivity analysis for reentry flows with inherent and model-form uncertainties. Journal of Spacecraft and Rockets, Vol. 49, No. 2, pp. 193-206, 2012
[25] Lamorte N, Friedmann P P, Glaz B, et al. Uncertainty propagation in hypersonic aerothermoelastic analysis. Journal of Aircraft, Vol.51, No. 1, pp. 192-203, 2014
[26] Danowsky B P, Chrstos J R, Klyde D H, et al. Evaluation of aeroelastic uncertainty analysis methods. Journal of Aircraft, Vol.47, No. 4, pp. 1266-1273, 2010
[27] Smolyak S. Quadrature and interpolation formulas for tensor products of certain classes of functions. Doklady Akademii Nauk Sssr. Vol.4, No.5, pp. 240-243, 1963
[28] Gerstner T, Griebel M. Numerical integration using sparse grids, numerical algorithms. Numerical Algorithms, Vol.18, No.3-4, pp.209-232, 1998
[29] Bungartz H J, Griebel M. Sparse grids. Acta Numerica, Vol.13, pp.147-269, 2004
[30] Xiong F, Greene S, Chen W, Xiong Y, Yang S. A new sparse grid based method for uncertainty propagation. Structural & Multidisciplinary Optimization, Vol.41, No.3, pp.335-349, 2009
[31] Wei Li, Zhenzhou Lu, Changcong Zhou. Importance analysis for models with dependant input variables by sparse grids. Journal of Aerospace engineering, Vol.228, No.10, pp.1875-1889, 2014
[32] Sobol I. Global sensitivity indices for nonlinear mathematical models and their monte carlo estimates. Mathematics and Computers in Simulation, Vol. 55, No,1-3, pp. 271–280, 2001
[33] Bungartz H J, Griebel M. Sparse grids. Acta Numerica,Vol.13, pp.147-269.2004
[34] He J, Gao S, Gong J, A sparse grid stochastic collocation method for structural reliability analysis. Structural Safety, Vol.51, pp. 29–34, 2014
[35] Liu Q, Ding L, Liu Q. A sparse grid method for the navier–stokes equations based on hyperbolic cross †. Mathematical Methods in the Applied Sciences, Vol. 37, No.6, pp. 870–881.2014
[36] Van Dyke M D. A study of second-order supersonic flow theory, Technical Report Archive & Image Library. 1081, NACA, 1951.
[37] Liu D D. Yao Z X. Sarhaddi D. Chavez F. From piston theory to a unified hypersonic-supersonic lifting surface method. Journal of Aircraft, Vol.34, No.3, pp.304-312,1997
[38] Zhang W W, Ye Z Y, Zhang C A et al. Analysis of supersonic aeroelastic problem based on local piston theory method. AIAA Journal, Vol.47, No.10, pp. 2321-2328,2009

Copyright Issues

Contact Author Email Address

Kun Ye: yekun@mail.nwpu.edu.cn
Zhengyin Ye: yezy@nwpu.edu.cn
Zihang Chen: chen10479@126.com
Zhan Qu: zhqu@xsyu.edu.cn